RES MILITARIS
REVUE EUROPEENNE D ETUDES EUROPEAN JOURNAL OF MILITARY STUDIES
Social Science Journal

Constructive Analysis on Aluminium - Nano Iron Composite during Cold Upsetting

By

P. Muthuraman
Department of Mechanical Engineering, Dhaanish Ahmed College of Engineering, Padappai, Tambaram, Chennai – 601301, India
E-mail: muthu_ab@yahoo.co.in

K. Karunakaran
Associate Professor, Department of Mechanical Engineering, Vel's Institute of Science Technology and Advance Studies, Deemed University, Vel's University, Tamil Nadu, India
Email id: kkaran.se@velsuniv.ac.in

Abstract

Formability and strain hardening are significant phenomena that are necessary to understand the plastic deformation phase of any material. They are also a key factor in understanding the workability requirements for metals. This study was done to evaluate the strain hardening as well as formability phenomenon that happens when sintered aluminum-nano iron powder composites are cold worked. Formability index increases quickly during the initial stage of deformation, followed by a slow rise when real axial strain grows further. Furthermore, it has been discovered that higher iron addition results in higher values of formability index. Also, the coefficients of rapid density Bi & Ci of the proposed aluminium ferrous composite preforms were being investigated and assessed analytically.

Key words: Sintered aluminum iron composites; Nano powders; upsetting; neural network;

1.0 Introduction

In the age of industrial integration, applications of nanotechnology include photoelectric, medical research, agricultural, energy, aircraft, materials, military and more [1]–[5]. Due to its enormous specific surface area, materials with substantial surface activity, high diffusing rate, and quantum effects are widely employed in highly effective recorded materials, electromagnetic fluid, absorbent materials, conduction paste, and nano-directing agents. Traditional industries have employed nano-sized metal powders extensively in recent years, spanning healthcare diagnosis, sun protection products, dyes, paints, and cosmetics [6]-[7].

In order to assess the work hardening characteristics, extensive study was done on both the iron composite with sintered aluminum-performs over uniaxial stress state conditions [8]-[12] the work hardening properties must be calculated. On work hardening, the impact of iron content, iron particle size distribution, and initial aspect ratio of the preforms was investigated. There is still more research to be done on the idea of distortion and fracture behaviour of powder metal preform. Therefore, an effort has been made in this study to determine the impact of Aluminium with nano iron composite preforms' ability to be formed depends on the amount of iron in them [13]-[16].

2. Experimental Analysis

Metal Powder Company in Madurai, India, then US Research Nano materials INC, USA provided the atomized aluminium and nano iron powders, respectively. Table 1 lists the characteristics of the powders. The treaties with different initial aspect ratios (i.e. height/diameter ratios), explicitly 0.45 and 0.75, were made in a hydraulic testing equipment with a capacity of 1000kN with a compacting pressure of 240 - 40 MPa. Each of these was created with three distinct iron content percentages (11, 21 and 31 per cent). When making the compacts, molybdenum disulphide (MoS_2) acted as a lubricant on to the punch, die and butt to condense friction. To prevent oxidation on the compacts' surface during sintering, a ceramic coating was added to it. The ceramic-coated compacts were sintered for 60 minutes in a dry, sand-filled container at 525°C in an electric muffle furnace. The compacts were endorsed to furnace equable to room temperature following the conclusion of the sintering programme. As soon as the compacts reached room temperature, the lasting ceramic coatings were detached using emery paper of available in various grades. A digital vernier calliper was used to measure the beginning heights and diameters. Mirror-polished flat dies were used in a 1000kN hydraulic press for the compression test.

To enable almost idle deformation, molybdenum disulphides were used as grease between the work tool and compacts. . Figure 1 shows EADX sample and its experimented samples are given in figure 2. Compressive loading was applied to each compact in increments of 0.01MN until the free surface started to show signs of cracking. One can see the fissures with the naked eye. Each of the deformed compacts had its height, interaction diameters (from top and bottom), expanded diameter and relative density noted immediately after each phase of the loading. The Archimedes principle, which is described elsewhere [17]-[19], can be used to compute the relative density. Figures 3 and 4 depict aluminium and iron samples captured by a SEM.

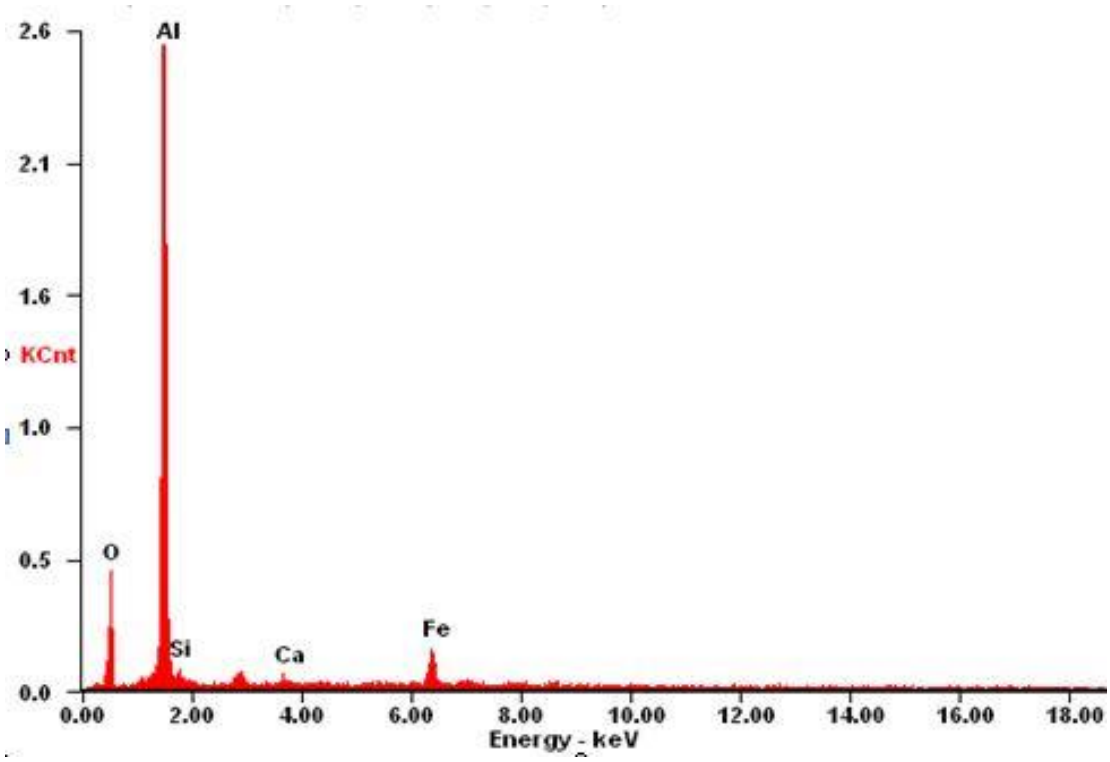

Figure 1 *EDAX of sample*

Figure 2 *Experimented Samples*

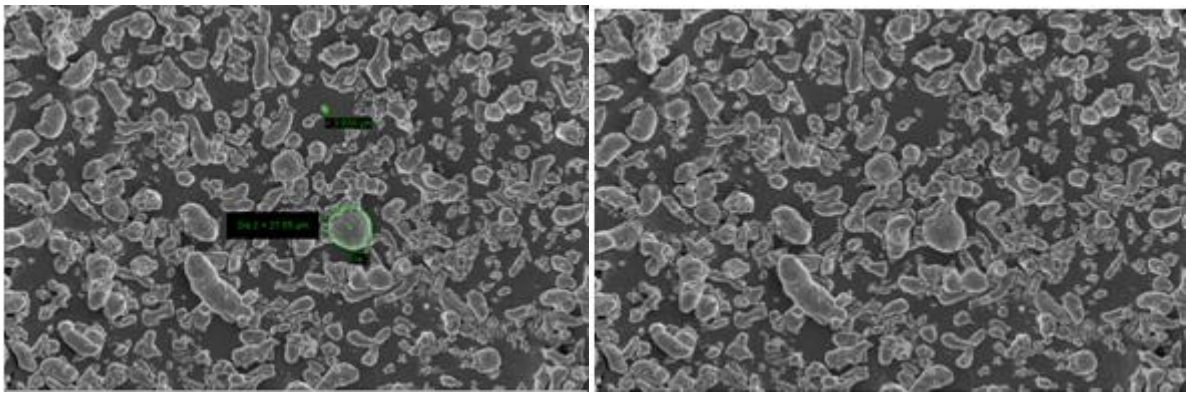

(3a) (3b)

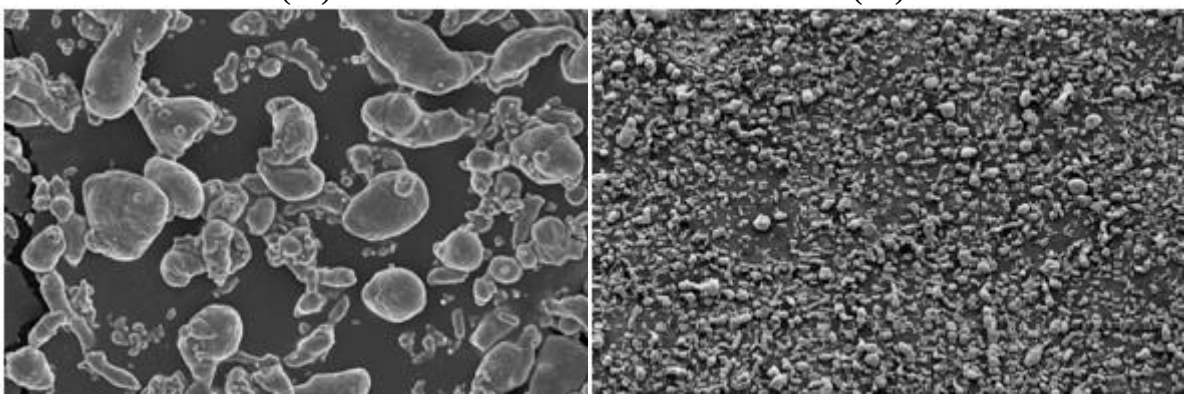

(3c) (3d)

Figure 3 *SEM morphology of aluminium powder*

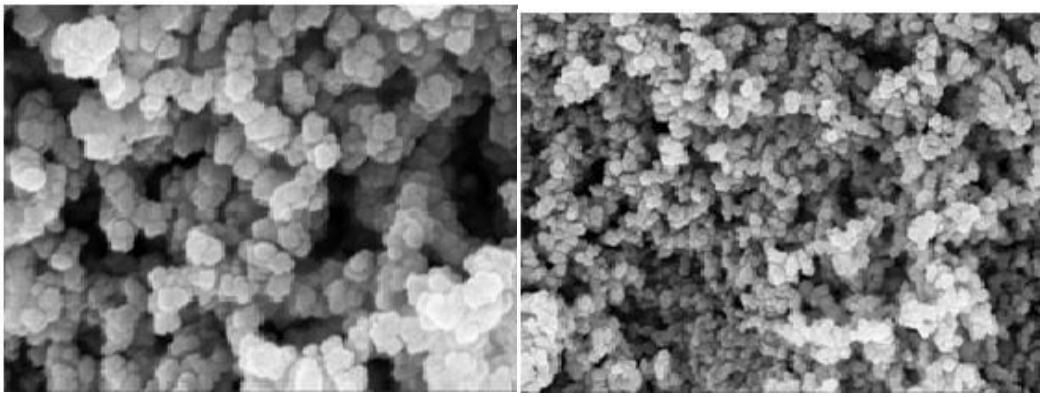

Figure 4 *SEM morphology of iron powder*

Table 1 *Characteristic of Aluminium and Nano iron powder*

Characteristics	Al	Fe
Actual density	1.03	2.87
Flow rate (S) (50g)	32.00	28.00
Compressibility	2.34 (310 Mpa)	6.69 (420 MPa)

3. Finite Element Analysis

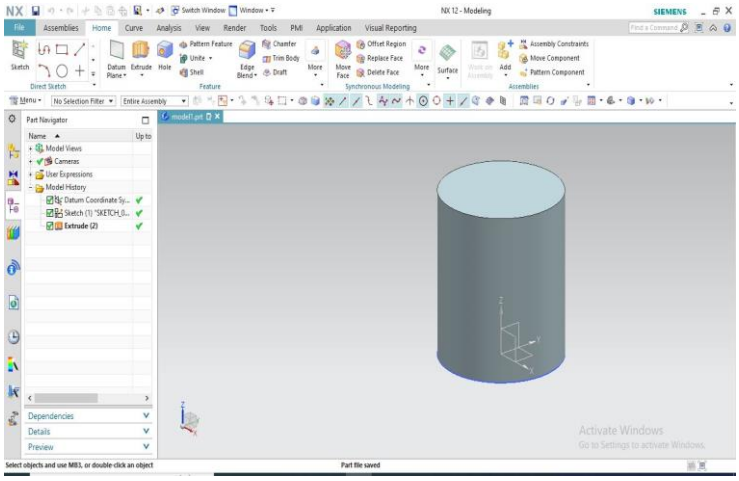

Figure 5 *Model for Analysis*

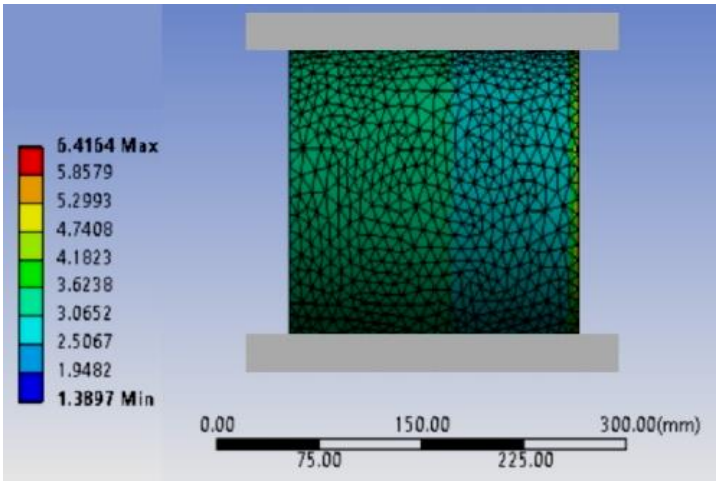

Figure 6 *Plot between Axial Stress vs Axial Strain*

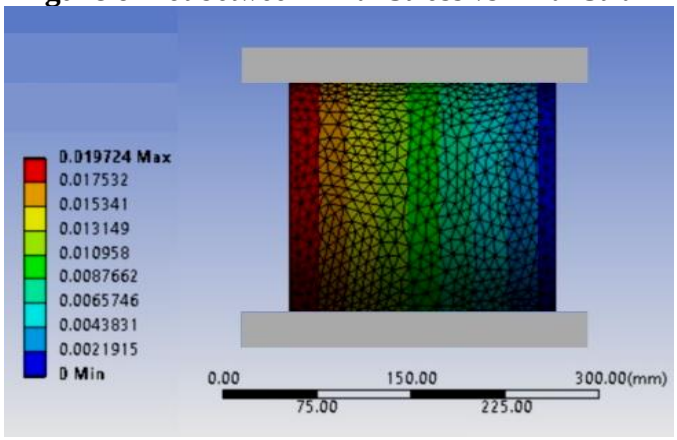

Figure 7 *Plot between Hoop Stress vs Axial Strain*

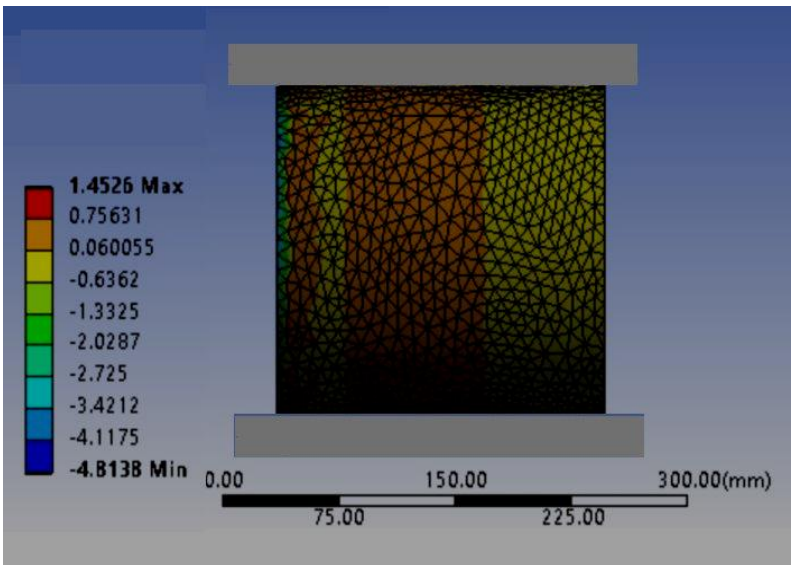

Figure 8 *Formability Index vs Axial Strain*

4. Results and Discussion

The suggested network model's process simulation capabilities are used to further evaluate how element size and ferrous content affects the formability which is shown in figure 5. Axial stress and axial strain have been plotted in Figure 6 for the preforms by an initial aspect ratio of 0.45 for various ferrous content percentages. When iron is added to an alloy, It is acknowledged that the values of the flow stress with axial strain rise. It has been discovered that axial stress rises quickly during the initial necking stages before rising gradually as genuine axial strain grows. This is as a result of the preforms' lateral distortion.

The Hoop stress and axial strain are depicted in Figure 7 for various iron concentrations with a 0.45 starting aspect ratio. It is noted that increased fracture strain is found when ferrous component in the aluminium with iron composite gets decreased. The reason for this is that there are fewer pores, which increases the fracture strain.

Using a starting aspect ratio of 0.45, Figure 8 depicts the correlation between the formability index besides various iron concentrations under axial strain. This graph demonstrates how axial strain causes an growth in the formability index. The large number of apertures linked to hydrostatic stress and higher iron content (30%) produce a superior formability index than lesser iron content, it is also highlighted.

Axial strain and density ratio are analyzed for various ferrous concentrations with an opening aspect ratio of 0.45. This demonstrates how the density ratio rises as the axial strain does. Furthermore, it is discovered that, as long as the aspect ratio is maintained, preforms with greater iron contents exhibit better density ratio values than those with lower iron contents (10%). This is because preforms with lower iron contents densify more uniformly than preforms with greater iron contents.

For varied ferrous concentrations with an opening aspect ratio of 0.45, are also constructed to know about the association between the immediate strain hardening exponent ni in addition the coefficient of strength Ki against axial strain, respectively. At great strain values, it was observed that the exponent ni and the strength coefficient Ki peak and begin to decline. Moreover, it is implied that iron (30%) has greater Ni and Ki values.

For various ferrous content proportions with an initial aspect ratio of 0.45, the defining characteristics of the instantaneous density of power law exponent Bi & the density constant Ci versus axial strains were studied. Exponent Ci is seen to peak and then decline at high strain values. When the material near the pore becomes more resistant to shape change due to work hardening, the matrix material need drift around the pores, which causes lateral spread. Additionally, it indicates how the exponent Bi rapidly rises as the true stature strain rises, peaks and then varies at peak strain values. It was clear that higher iron contents (10%) have higher Ci standards, whereas the opposite is true for the density power law exponent Bi.

5. Conclusion

In this paper, a constructive study of aluminum-nano iron composites has been completed. The samples under investigation contain aluminium composites with various iron contents of 11, 21, and 31% and two distinct aspect ratios of 0.45 and 0.75. The findings of the finite element analysis and upset forging experimental analysis are provided above. It can be deduced from both experiments that, for the same aspect ratio (0.45 or 0.75), an increase in the iron content (30wt%) results in an increase in the value of formability index, a decrease in fracture strain, an improvement in the density ratio, a higher exponent of strain hardening and a rise in coefficient of strength.

Appendix

Nomenclature

D_0 initial diameter of the preform
D_b bulged diameter of the preform after deformation
D_c contact diameter of the preform after deformation
h_0 initial height of the cylindrical preform
h_f height of the barreled cylinder after deformation
ε_z true strain in the axial direction
ε_θ true strain in the hoop direction
σ_z true stress in the axial direction
σ_θ true stress in the hoop direction
σ_m hydrostatic stress

conventional Poisson's ratio

β Formability index
k_i instantaneous strength coefficient
n_i instantaneous strain hardening exponent
B_i instantaneous density coefficient
C_i instantaneous density coefficient

List of tables and figures

Figure 8 : Formability Index vs Axial Strain

References

R.Narayanasamy and R.A.Ponalagusamy, Mathematical theory of plasticity for compressible powder maetallurgy materials – Part II, International Journal of material processing and technology, 97 (2000) 110-113.

Green RJ, A plasticity theory for porous solids, International Journal of Mechanical Sciences, 149 (1972) 214-224.

Shima S, Oynae M, Plasticity theory for porous metals, International Journal of Mechanical Sciences, 18 (1976) 285-291.

Lee DN and Kim HS, Plastic yield behavior of porous metals, International Journal of powder Metallurgy, 35 (1992) 275-279.

K.P.Rao and E.B.Hawbolt, Development of constitutive relationships using compression testing of medium carbon steel, Journal of Engineering Material Technology transactions, ASME 114 (1992) 116-123.

Weng TL and Sun CT, A study of fracture criteria for ductile materials, Engineering Failure Analysis, 7 (200) 101-125.

V Tvergaard, On localization in ductile materials containing spherical voids, International Journal of Fracture,18/4 (1982) 237-252.

B.P.P.A Gouveia, J.M.C. Rodrigues and P.A.F.Martins , Ductile fracture in metal working experimental and theoretical research, International Journal of Material Processing Technology, 101 (2000) 52-63.

A.Venugopal Rao, N.Ramakrishnan and R.Krishnakumar, Comprehensive evaluation of the theoretical failure criteria for workability in cold forging, International Journal of Material Processing Technology, 142 (2003) 29-42.

J.J. Park, Constitutive relations to predict plastic deformations in porous metal during compaction, International Journal of Mechanical Sciences, 37 (1995) 709-719.

Petruska J and Janicek L, Coputationally experimental workability determination of compressed cylindrical specimen with surface defect, International Journal of Material Processing Technology, 80-81(1998) 572-578.

R.Narayanasamy, T.Ramesh and K.S.Pandey, Some aspects on workability of aluminium – iron powder metallurgy composite during cold upsetting, International journal of Material Science Engineering, A391 (2005) .418-426.

N.Selvakumar, R.Narayanasamy, Phenomenon of strain hardening behaviour of sintered aluminium preforms during cold axial forming, Journal of Material Processing Technology, 142 (2) (2003) 347-354.

K. N. Devi, J. Anand, R. Kothai, J. M. Ajai Krishna, and R. Muthurampandian, “Sensor based Posture Detection System”, Materials Today Proceedings, 55 (2), 359-364, 2022.

Jose A., K. N. Devi, Z. E. Kennedy, and R. Dhanalakshmi, “Processing Techniques for Sensor Materials: A Review”, Materials Today Proceedings, 55 (2), 430-433, 2022.

R. Narayanasamy and R. Ponalagusamy, “A Mathematical theory of plasticity for compressible powder metallurgy materials – Part II”, International journal of Material Processing Technology, 97 (2000) 110-113.

N.Selvakumar, P.Radha ,R.Narayanasamy and P.Ganesan, Neural network model for predicting strain hardening and densification constants of sintered aluminium preforms, Powder Metallurgy,47(3) (2004) 261-266.

The MathWorks, Inc., Neural Network Toolbox for use with Matlab 5.3, Natick, MA,1998.

Rajkumar Vaidyanathan and Nilay Papila, Neural network and response surface methodology for rocket engine component optimization, AIAA NASA (4880) (2000) 1-21.